Article

Discovery Medicine 2026; 38(206): 687–694
https://doi.org/10.24976/Discov.Med.202638206.57

Anti-Inflammatory Therapeutic Effect of Tegoprazan in Spinal Cord-Injured Rats

Min Je Kim[1,†], Seong Jun Kim[1,†], Daye Lee[1], Gi-Beom Ju[1], Gong Ho Han[1], Wan-Kyu Ko[2], Je Beom Hong[3], Min Jai Cho[4,*], Seil Sohn[1,5,*]

[1]Department of Life Science, CHA University, 13488 Seongnam-si, Gyeonggi-do, Republic of Korea
[2]Department of Chemistry and Chemical Biology, Rutgers, The State University of New Jersey, Piscataway, NJ 08854, USA
[3]Department of Neurosurgery, Kangbuk Samsung Hospital, Sungkyunkwan University School of Medicine, 03181 Seoul, Republic of Korea
[4]Department of Neurosurgery, Chungbuk National University Hospital, Chungbuk National University College of Medicine, 28644 Cheongju-si, Chungcheong-do, Republic of Korea
[5]Department of Neurosurgery, CHA Bundang Medical Center, 13496 Seongnam-si, Gyeonggi-do, Republic of Korea
*Correspondence: ulbo811211@naver.com (Min Jai Cho); sisohn@cha.ac.kr (Seil Sohn)
[†]These authors contributed equally.
Submitted: 27 November 2025 Revised: 19 January 2026 Accepted: 13 February 2026 Published: 20 March 2026

Background: Spinal cord injury (SCI) can induce secondary damage, such as inflammation, oxidative stress, and neuronal cell death. These factors impede recovery. This study evaluated the therapeutic potential of tegoprazan (TEGO), a drug known to act via a potassium-competitive acid blocker, in a SCI rat model.

Methods: We conducted SCI in female rats, and TEGO was administered intraperitoneally. Methylprednisolone (MP) was used as a positive control. TEGO was dissolved in dimethyl sulfoxide (DMSO) and sonicated before injection. Toxicity was assessed by body weight monitoring, and motor recovery was assessed by behavioral tests. We performed immunofluorescence and qRT-PCR to investigate inflammatory markers. Western blot analyses were evaluated for mitogen-activated protein kinase (MAPK) and nuclear factor kappa B (NF-κB) signaling pathways.

Results: TEGO treatment had no systemic toxicity and improved motor recovery. TEGO ($p < 0.05$) and MP ($p < 0.01$) decreased inducible nitric oxide synthase (iNOS) expression. CD206 expression was significantly increased in the MP group ($p < 0.01$) compared with the Vehicle group, whereas the TEGO group showed a slight increase compared with the Vehicle group. Furthermore, TEGO inhibited MAPK/NF-κB signaling, attenuating pro-inflammatory cytokine production.

Conclusions: TEGO, a representative potassium-competitive acid blocker (P-CABs), suppressed pro-inflammatory gene expression and might be applied as a novel treatment for SCI.

Keywords: SCI; TEGO; P-CABs; voltage-gated potassium channel 1.3

Introduction

Spinal cord injury (SCI) causes marked neuropathology, involving limited functional recovery [1]. In addition, SCI is known to trigger secondary pathological responses following the initial trauma, including inflammation, oxidative stress, and neuronal apoptosis [2,3]. Many researchers have tried to reduce secondary damage through inflammatory responses following SCI [4].

Among therapeutic strategies, a high dose of methylprednisolone (MP) has been used for its potent anti-inflammatory effects [5–7]. However, such high-dose MP treatments cause side effects such as headache and muscle weakness [5,8].

Tegoprazan (TEGO), a potassium-competitive acid blocker (P-CABs), is primarily applied to reduce gastric acid secretion and has been approved in South Korea as a treatment for gastroesophageal reflux disease (GERD), infections, and gastric ulcers [9]. TEGO, a representative P-CAB, is known not only to suppress gastric acid secretion but also to exhibit potential anti-inflammatory effects [10].

In one study, P-CABs were reported to regulate inflammatory responses through the p38 and c-Jun N-terminal kinase (JNK) pathways among the mitogen-activated protein kinase (MAPK) signaling pathways [11].

In addition, voltage-gated potassium channel 1.3 (Kv1.3) overexpression induced pro-inflammatory cytokine expression, the phosphorylation of extracellular signal-regulated kinase (ERK), and nuclear factor kappa B (NF-κB) in macrophages [12]. A Kv1.3 blockade was found to suppress inflammatory microglial activation and cytokine secretion via the NF-κB signaling pathway [13]. These findings designate the ERK and NF-κB pathways as downstream regulators of Kv1.3.

A study has also noted the anti-inflammatory effect of TEGO, evaluated using LPS (Lipopolysaccharide)-

stimulated BMM (Bone Marrow-Derived Macrophages) macrophages *in vitro* [11]. The present authors evaluated the anti-inflammatory effects of TEGO in a SCI rat model.

Materials and Methods

Preparation and Characterization of TEGO and MP

TEGO was obtained from HK Inno. N Corporation (Seoul, Korea) and solubilized in dimethyl sulfoxide (DMSO, Tokyo Chemical Industry Co., Tokyo, Japan). The MP was obtained from Reyon Pharm in Seoul, Korea, and was used without further modification.

In Vivo Toxicity Study

All animal-related procedures complied with the requirements of the CHA University Institutional Animal Care and Use Committee (IACUC240101) and followed the NIH's guidelines for the care and use of laboratory animals. Housed in a facility at 55–65% humidity and a controlled temperature of 24 ± 3 °C with a light/dark cycle of 12 h, and given free access to water and food [14]. Female Sprague-Dawley (SD) rats (180–200 g, Raon Bio Co., Gyeonggi-do, Korea) were divided into DMSO (n = 5) and TEGO (n = 5). To assess acute toxicity, rats in the TEGO group received a single intraperitoneal (i.p.) injection of TEGO (30 mg/kg) dissolved in DMSO. The control group received a single i.p. injection of an equivalent volume of DMSO alone [15,16]. To evaluate biodistribution and body weight changes, we observed abnormal behavior, toxic symptoms, body weight, and death for 14 consecutive days [17–19].

Surgical Procedures

Anesthesia was administered prior to surgery. Rats were anesthetized via an intraperitoneal injection of a combination of Zoletil® (50 mg/kg, Virbac Laboratories, Carros, France) and Rompun® (10 mg/kg, Elanco Korea, Seoul, Korea). The T8–T10 region was exposed, and a total laminectomy at T9 was performed to reveal the spinal cord [20]. Contusion SCI was induced by applying a metal weight (40 g, 2.5 mm diameter) for 5 s using an impactor (RWD, CA, USA), thereby inducing a standardized contusion injury [20]. A total of 27 rats underwent spinal cord injury surgery and were randomly assigned to three groups (Vehicle, MP, and TEGO; n = 9 per group). The vehicle, MP, and TEGO groups received a single i.p. injection immediately after injury (MP: 30 mg/kg, TEGO: 30 mg/kg). We randomly divided all rats (n = 27) into three groups: the Vehicle group (injury + Vehicle, n = 9), the MP group (injury + MP, n = 9), and the TEGO group (injury + TEGO, n = 9). The experimental endpoint was set to 14 days post-injury. All animals were euthanized simultaneously on day 14. Three rats per group on predetermined days were anesthetized. After cannulation of the left ventricle-ascending aorta, rats were sacrificed by intracardiac perfusion with saline for IF staining (n = 9). The other six rats per group were euthanized by CO2 asphyxiation, and the spinal cords were removed for qRT-PCR (n = 3) and Western blot assays (n = 3) [19,21].

Experimental Groups and Hindlimb Locomotor Assessment

The vehicle, MP, and TEGO groups received a single i.p. injection immediately after injury. Motor function was assessed independently by two evaluators who were unaware of the group assignments. The final score was calculated as the mean of assessment results. To assess hindlimb motor function, we assessed the Basso, Beattie, and Bresnahan (BBB) score. The BBB motor rating scale was previously described in our studies [22,23]. The rats were evaluated on days 1, 3, 7, and 14 after injury.

IF Staining of GFAP, iNOS, and CD206

The spinal cords were embedded in paraffin and prepared for IF staining. We stained the markers Glial fibrillary acidic protein (GFAP), inducible nitric oxide synthase (iNOS), and cluster of differentiation 206 (CD206) using commercially available primary antibodies (GFAP, mouse, Invitrogen; iNOS, rabbit, Abcam; CD206, goat, R&D Systems), as described in our previous study [24]. These procedures and methods were provided in the **Supplementary Material**. For IF staining, longitudinal spinal cord sections (5 µm thick) were collected from three rats per group along the dorsoventral axis. We randomly and blindly selected three square areas (33 × 33 µm, for a total of twelve images/group) in the region of interest (ROI,270 × 270 µm) under × 400 magnification. The ROI was quantified using the ImageJ software package (version 1.54g; National Institutes of Health (NIH), Bethesda, MD, USA).

qRT-PCR

The spinal cord was collected 10 mm in length, including the lesion center. The segments were homogenized using TRIzol reagent (Invitrogen, Cat # 15596018, Carlsbad, USA) for RNA extraction. We synthesized Complementary DNA (cDNA) as previously described [24]. We assessed the relative expression levels of the inflammatory markers (Tumor necrosis factor-α (TNF-α), IL-1β, IL-6, and iNOS), the anti-inflammatory markers (CD206, arginase-1 (Arg-1), and IL-10), and normalized them to the expression level of glyceraldehyde-3-phosphate dehydrogenase (GAPDH) [25]. Detailed primers and methods for the qRT-PCR are explained in the **Supplementary Material**.

Western Blotting

Thirty µg of protein samples in equal volumes were subjected to sodium dodecyl sulfate-polyacrylamide gel electrophoresis (SDS-PAGE) and transferred to polyvinylidene difluoride (PVDF) membranes [26]. The western blot procedures and methods were provided in the **Supplementary Material**. We used β-actin as an internal control. The

phosphorylation levels of ERK, JNK, and p38 were compared between groups by normalizing the p/t ratio to 1 in the Vehicle group. The volumes of the phosphorylated and total forms (p/t form) were quantified by ImageJ.

Statistical Analyses

One-way analysis of variance (One-way ANOVA) was used for multiple comparisons among groups. Tukey's multiple-comparison test was used as a post hoc analysis method. Differences in *p*-values were considered statistically significant for which $*p < 0.05$, $**p < 0.01$, and $***p < 0.001$; ns, not significant. All statistical analyses and graphing were performed using GraphPad Prism (version 9.5.0 (730); GraphPad Software, San Diego, CA, USA).

Results

Evaluation of Systemic Toxicity Following I.P. Administration of TEGO

Following an I.P. administration of TEGO (30 mg/kg), there were no mortality events or clinical signs of acute toxicity in rats as determined by their consistent body weight, unaltered behavioral patterns, and lack of abnormalities in the emesis, fecal output, and urinary excretion (Fig. 1). Unaltered behavioral patterns and abnormalities in the emesis, fecal output, and urinary excretion were not observed. An autopsy revealed no abnormalities in the organs (**Supplementary Fig. 1**).

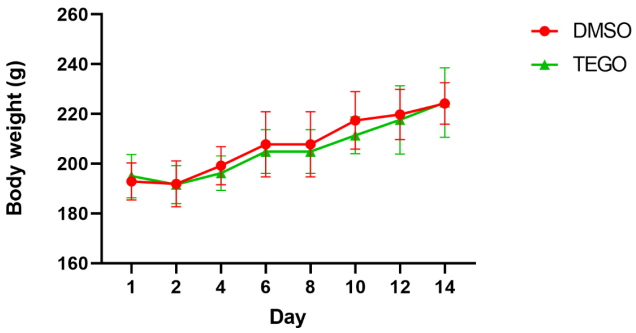

Fig. 1. Morphological evaluation of potential toxicity following intraperitoneal (i.p.) injection. Body weight changes in Sprague-Dawley (SD) rats after administration of tegoprazan (TEGO, 30 mg/kg, i.p., n = 5). No apparent morphological abnormalities or organ damage were observed (**Supplementary Fig. 1**).

TEGO Enhanced Behavioral Recovery in the SCI Rats

We evaluated motor function using the BBB hindlimb locomotor rating scale on days 1, 3, 7, and 14 (Fig. 2). On day 3, there were no differences in the motor function among all groups, while the MP group showed improved motor function compared to the vehicle group on day 7. On day 14, motor function in both the MP and TEGO groups was improved compared to the Vehicle group. There were no significant differences in motor function between the MP and TEGO groups.

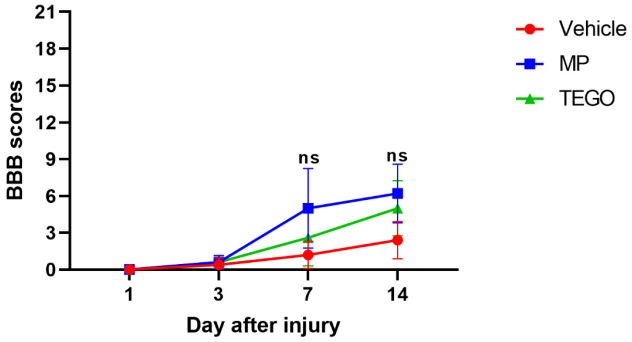

Fig. 2. A comparison of motor functional recovery was conducted using Basso, Beattie, and Bresnahan (BBB) locomotor scores among the Vehicle (n = 5), methylprednisolone (MP, n = 5), and TEGO (n = 5) groups. The BBB scores were assessed for 14 days following spinal cord injury (SCI). A one-way ANOVA followed by a Tukey test was used to determine the existence of significant differences among groups. ns indicates no statistically significant difference.

TEGO Inhibited the Expression of Inflammatory Markers in the Histological Analysis

To determine the anti-inflammatory effect of TEGO on tissues after SCI, we conducted an IF evaluation using inflammatory (iNOS) and anti-inflammatory (CD206) macrophage markers. Fig. 3 presents differences in iNOS expression levels at 14 days after SCI (Fig. 3a–l). In the vehicle group, the iNOS/DAPI fluorescence intensity was measured. The MP group was significantly reduced compared to the vehicle group (MP: $p < 0.01$). The TEGO group was also significantly decreased compared to the vehicle group (TEGO: $p < 0.05$). However, there was no significant difference between the MP and TEGO groups (Fig. 3m). Fig. 4 shows the differences in CD206 expression levels between the groups 14 days after SCI (Fig. 4a–l). In the vehicle group, the CD206/DAPI fluorescence intensity was assessed. The expression of CD206 in the MP group ($p < 0.01$) was significantly increased compared to that in the vehicle group.

TEGO Reduced Inflammatory Cytokines Gene Expressions

The gene expression levels of inflammatory cytokines are shown in Fig. 5a–d. The expression levels of IL-6, IL-1β, iNOS, and TNF-α were highest in the Vehicle group. IL-6 expression was significantly reduced in the MP and TEGO groups (MP: $p < 0.01$; TEGO: $p < 0.01$). IL-1β expression was significantly suppressed in the MP and TEGO groups (MP: $p < 0.001$; TEGO: $p < 0.001$). iNOS ex-

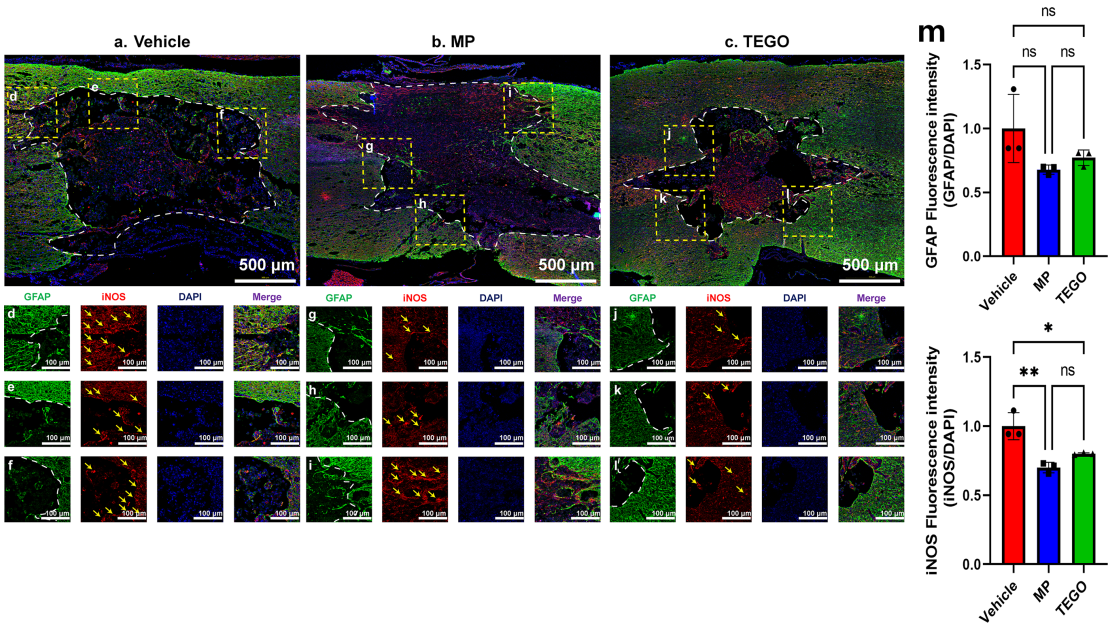

Fig. 3. The immunofluorescence (IF) staining of anti-glial fibrillary acidic protein (GFAP, Green) and anti-inducible nitric oxide synthase (iNOS, Red) in the spinal cord lesion area. Representative merged image for GFAP and iNOS of the Vehicle, MP, and TEGO groups following SCI (a–c, Scale bar: 500 μm). Three areas are the enlarged images of the area around the damage boundary in (d–f) Vehicle (n = 3), (g–i) MP (n = 3), and (j–l) TEGO (n = 3) groups (Scale bar: 100 μm). (m) Quantitative analysis of the GFAP and iNOS fluorescence intensity levels. Results are presented as the mean ± SEM from triplicate experiments (*p <0.05, **p < 0.01). ns indicates no statistically significant difference. The yellow arrows in Fig. 3 indicate fluorescent signals corresponding to adhesion molecule expression.

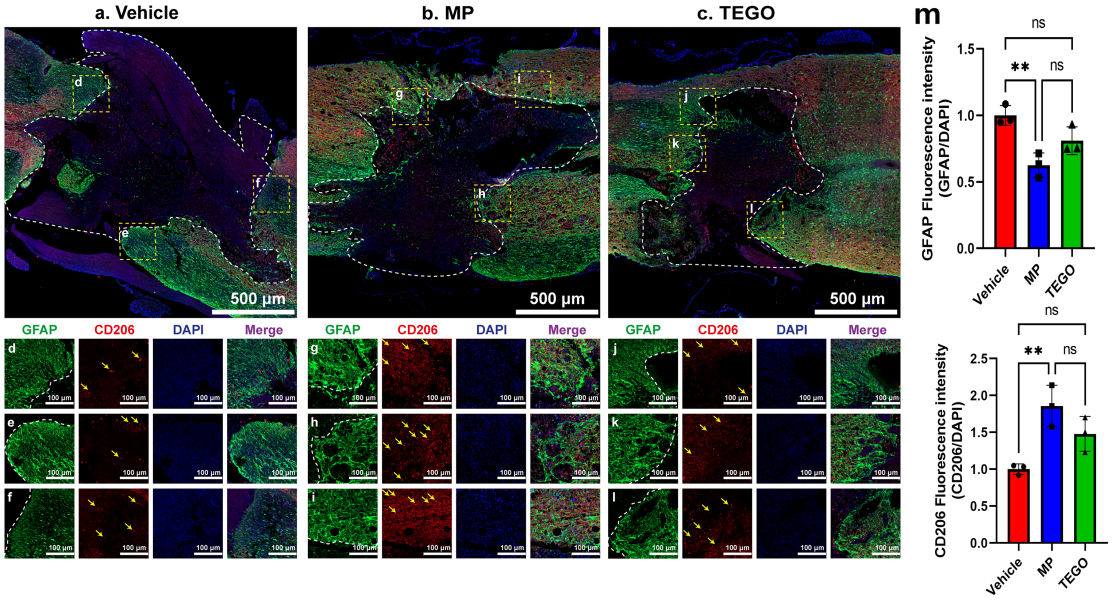

Fig. 4. The IF staining of GFAP (Green) and anti-cluster of differentiation 206 (CD206, Red). In the spinal cord lesion area. Representative merged image for GFAP and CD206 of the Vehicle, MP, and TEGO groups following SCI in the rat (a–c, Scale bar: 500 μm). Three areas are the enlarged images of the area around the damage boundary in (d–f) Vehicle (n = 3), (g–i) MP (n = 3), and (j–l) TEGO (n = 3) groups (Scale bar: 100 μm). (m) Quantitative analysis of the GFAP and CD206 fluorescence intensity levels. Results are presented as the mean ± SEM from triplicate experiments (**p < 0.01). ns indicates no statistically significant difference. The yellow arrows in Fig. 4 indicate fluorescent signals corresponding to adhesion molecule expression.

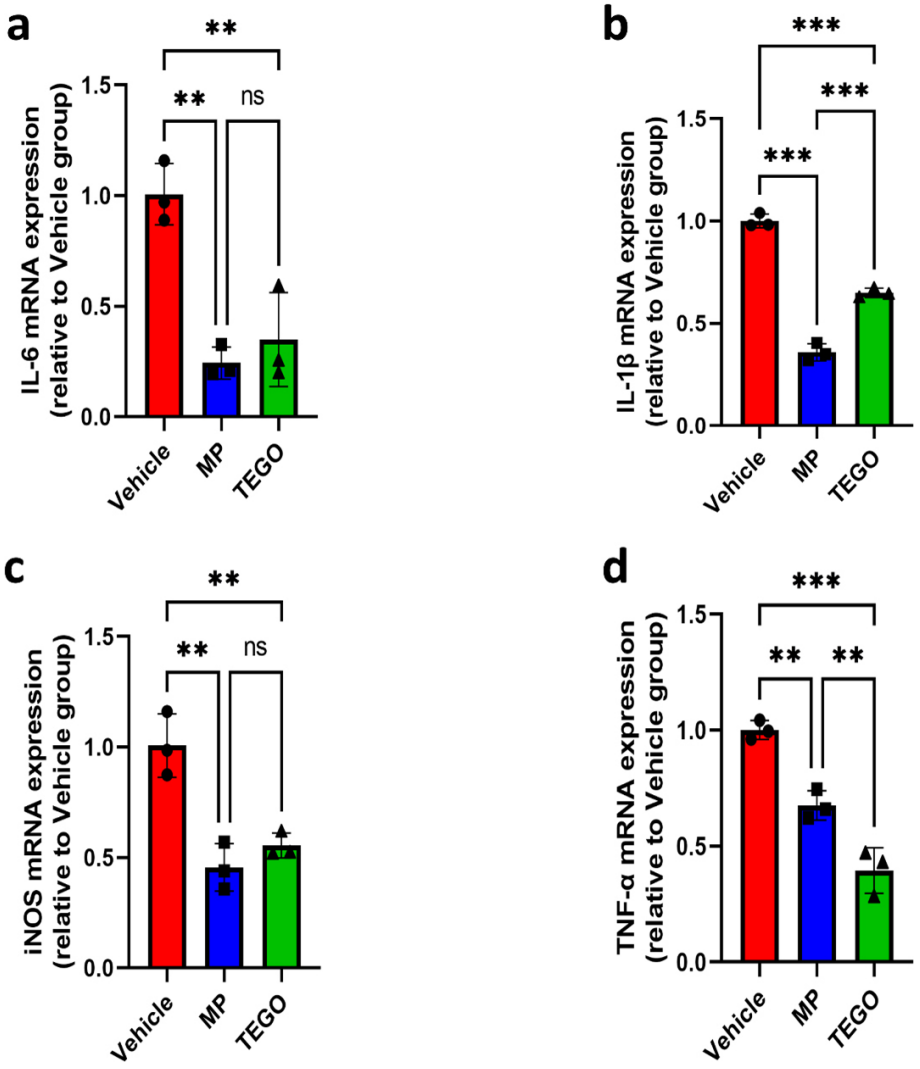

Fig. 5. Representative quantitative real-time polymerase chain reaction (qRT-PCR) showed the analysis of mRNA expression levels of the pro-inflammatory cytokine in injured spinal cord segments. Segments of the spinal cord (10 mm) were evaluated 14 days after injury. The relative expression levels of (a) interleukin-6 (IL-6), (b) IL-1β, (c) iNOS, and (d) Tumor necrosis factor-α (TNF-α) were evaluated in segments of the spinal cord with the lesion epicenter. The mRNA expression levels were normalized to the levels of glyceraldehyde 3-phosphate dehydrogenase (GAPDH). The results are presented as the mean $\pm$ SEM from triplicate experiments (n = 3, $^{**}p < 0.01$, and $^{***}p < 0.001$). ns indicates no statistically significant difference.

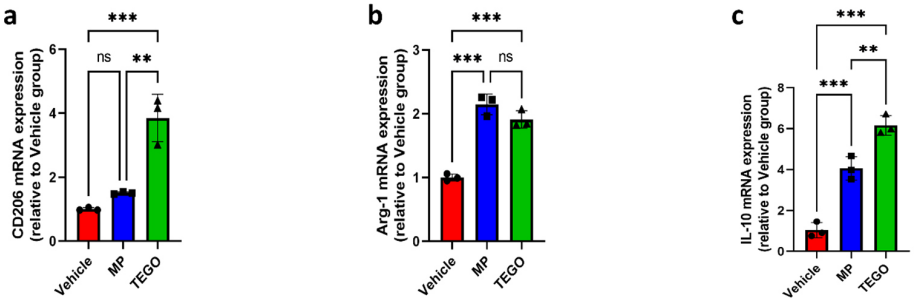

Fig. 6. Representative qRT-PCR showed the analyzed mRNA expression levels of the anti-inflammatory cytokine in injured spinal cord segments. The levels of relative expression of (a) CD206, (b) arginase-1 (Arg-1), and (c) IL-10 were normalized to GAPDH. The results are presented as the mean $\pm$ SEM from triplicate experiments (n = 3, $^{**}p < 0.01$, and $^{***}p < 0.001$). ns indicates no statistically significant difference.

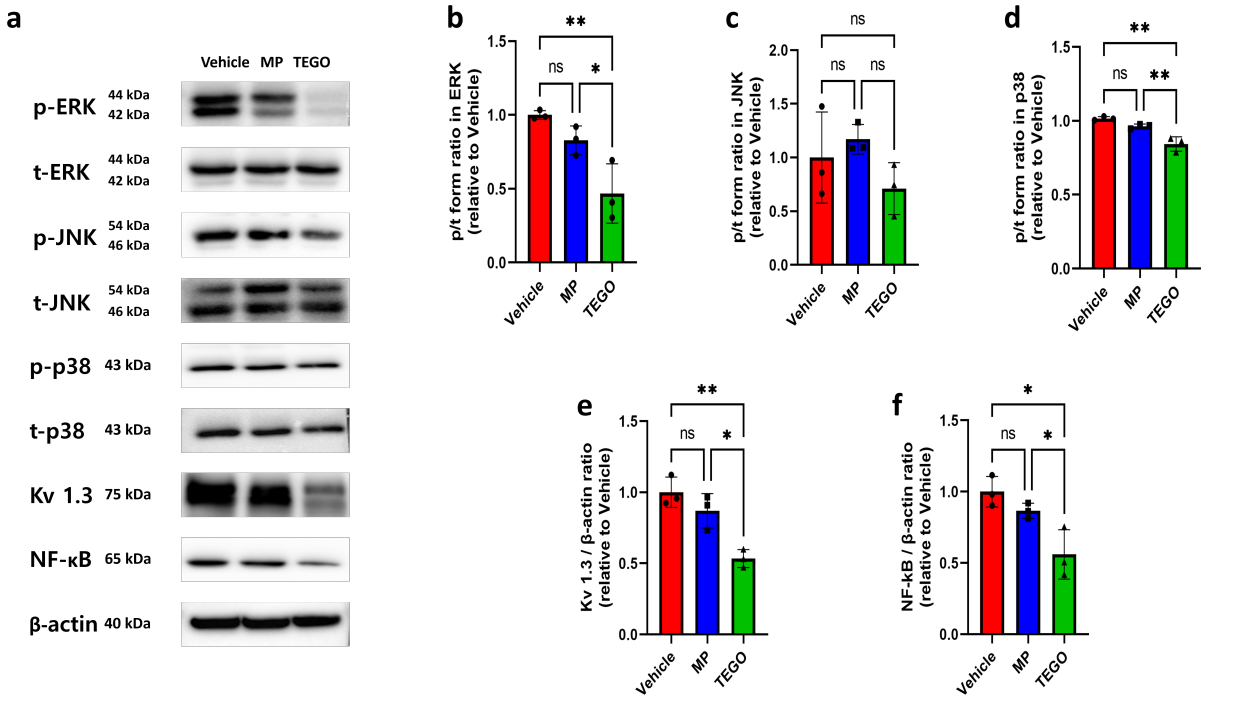

Fig. 7. Representative images and quantitative analyses of phosphorylation activities of the mitogen-activated protein kinase (MAPK) signaling pathway and voltage-gated potassium channel 1.3 (Kv1.3) in the Vehicle, MP, and TEGO groups. (a) Representative images. Quantitative analyses of phosphorylated/total (p/t) forms of (b) extracellular signal-regulated kinase (ERK), (c) c-Jun N-terminal Kinases (JNK), and (d) p38, (e) Kv1.3, (f) nuclear factor kappa B (NF-κB), and β-actin. The volume of the p/t form in the Vehicle group was set to one-fold and then quantified. The Kv1.3/β-actin and NF-κB/β-actin volumes in the vehicle group were set to one-fold and quantified. The results are the mean $\pm$ SEM of triplicate experiments (n = 3, *$p < 0.05$, and **$p < 0.01$). ns indicates no statistically significant difference.

pression was also decreased in the MP and TEGO groups (MP: $p < 0.01$; TEGO: $p < 0.01$). TNF-α expression levels were similar (MP: $p < 0.01$; Vehicle + TEGO: $p < 0.001$). The anti-inflammatory cytokine gene expression levels, in this case CD206, Arg-1, and IL-10, are shown in Fig. 6a–c. CD206 expression was significantly increased in the TEGO group ($p < 0.001$) but not in the MP group. The observed differences may be due to the fact that immunofluorescence (IF) staining and qPCR assess different levels of expression (protein localization versus mRNA expression). Arg-1 expression was significantly increased in the MP ($p < 0.001$) and TEGO ($p < 0.001$) groups, and IL-10 expression was significantly increased in the MP ($p < 0.001$) and TEGO ($p < 0.001$) groups.

TEGO Suppressed Inflammation Through the MAPK Signaling Pathway and Kv1.3 After SCI

The TEGO group showed a significant reduction in the expression of Kv1.3, accompanied by decreased phosphorylation levels of MAPK pathway markers (Fig. 7a–f). The MP treatment group showed no further activation compared to the Vehicle group of p-ERK, p-JNK, p-p38, NF-κB, and Kv 1.3 levels (Fig. 7b–f). Compared with the Vehicle and MP groups, the TEGO group showed significantly reduced expression levels of p-ERK (Vehicle: $p < 0.01$ and MP: $p < 0.05$), p-p38 (Vehicle: $p < 0.01$ and MP: $p < 0.01$), NF-κB (Vehicle: $p < 0.05$ and MP: $p < 0.05$), and Kv 1.3 (Vehicle: $p < 0.01$ and MP: $p < 0.05$), along with suppressed p-JNK expression, while there was not significant reduction in the p-JNK expression.

Discussion

We evaluated the therapeutic effects of TEGO, a P-CAB, in a rat SCI model. TEGO was found to promote functional recovery by suppressing inflammation and enhancing anti-inflammatory signaling. These effects were similar to those of MP, a standard anti-inflammatory agent used in SCI treatments. Although MAPK expression showed a decreasing trend in the MP group, the difference did not reach statistical significance. Previous studies indicate that MP-induced modulation of MAPK signaling is context-dependent, and the limited sample size in this study may have reduced the statistical power to detect subtle changes in MAPK signaling.

An analysis of BBB motor scores revealed that the TEGO treatment improved motor recovery 14 days after SCI (Fig. 2), consistent with modulation of inflammatory markers [27]. Notably, both TEGO and MP decreased GFAP and iNOS expressions and enhanced CD206 expres-

sion (Figs. 3,4). This suggests that TEGO can promote a shift toward an anti-inflammatory effect.

TEGO was shown to suppress the expression of inflammatory cytokines, in this case IL-1β, TNF-α, IL-6, and iNOS, while upregulating the expression of the anti-inflammatory cytokines IL-10, Arg-1, and CD206. Effects on microglia/macrophage polarization were also observed, a finding consistent with previous reports that macrophage phenotypes modulate SCI outcomes [28].

The consistency of the results of IF staining (Figs. 3,4), qPCR (Figs. 5,6), and Western blot analyses (Fig. 7) supports the conclusion that TEGO exerts potent immunomodulatory effects after SCI.

Recent evidence suggests that P-CABs possess anti-inflammatory properties and can thus modulate MAPK signaling pathways [11]. A blockade of Kv1.3 channels exerts its anti-inflammatory effects along the downstream MAPK (p38, JNK) and NF-κB signaling pathways. Consistent with the suppression of MAPK signaling observed in this study, the expression level of Kv1.3 was significantly decreased in the TEGO group compared to that in the Vehicle and MP groups. To the best of our knowledge, this is the first study to evaluate the anti-inflammatory effects of TEGO after SCI.

Despite these findings, the direct involvement of the Kv1.3 channel in the TEGO-mediated regulation of inflammatory cytokine production and MAPK signaling remains to be fully elucidated and requires further experimental validation [29]. In addition, further studies investigating the long-term safety, pharmacokinetics, and detailed molecular mechanisms of TEGO are necessary to establish its potential applicability as a novel therapeutic strategy for spinal cord injury.

Conclusion

TEGO, a representative P-CAB, reduced the expression of major pro-inflammatory genes. Based on the results here, TEGO can be suggested as a potential anti-inflammatory therapeutic agent for SCI. These results suggest that TEGO has anti-inflammatory properties and might be applied as a novel treatment for SCI.

Abbreviations

SCI, Spinal cord injury; TEGO, Tegoprazan; P-CABs, Potassium-competitive acid blocker; i.p, Intraperitoneal; MP, Methylprednisolone; DMSO, Dimethyl sulfoxide; IF, Immunofluorescence; qRT-PCR, Quantitative real-time polymerase chain reaction; iNOS, Nitric oxide synthase; Kv1.3, Voltage-gated potassium channel 1.3; MAPK, Mitogen-activated protein kinase; JNK, c-Jun N-terminal kinase; ERK, Extracellular signal-regulated kinase; NF-κB, Nuclear factor kappa B; GERD, Gastroesophageal reflux disease; IL-6, Interleukin-6; TNF-α, Tumor necrosis factor-α; IACUC, Institutional Animal Care and Use Committee; NC3Rs, National Centre for the Replacement, Refinement and Reduction of Animals in Research; SD, Sprague-Dawley; BBB, Basso, Beattie, and Bresnahan; GFAP, Glial fibrillary acidic protein; cDNA, Complementary DNA; Arg-1, Arginase-1; GAPDH, Glyceraldehyde-3-phosphate dehydrogenase; SDS-PAGE, Sodium dodecyl sulfate-polyacrylamide gel electrophoresis; iNOS, Nitric oxide synthase; CD206, Cluster of differentiation 206; One-way ANOVA, One-way analysis of variance.

Availability of Data and Materials

The data used to support the findings of this study are included within the article.

Author Contributions

MJK: conceptualization, methodology, investigation, and writing; SJK: validation, data curation, methodology, and review & editing; DL: validation, methodology, investigation, and review & editing; GBJ, GHH, WKK, and JBH: methodology and investigation, review & editing; MJC: supervision, investigation, review & editing, and funding acquisition; SS: conceptualization, writing, review & editing, funding acquisition, supervision, and project administration. All authors read and approved the final manuscript. All authors agreed to be accountable for all aspects of the work in ensuring that questions related to the accuracy or integrity of any part of the work are appropriately investigated and resolved.

Ethics Approval and Consent to Participate

This study was conducted according to the guidelines of the Institutional Animal Care and Use Committee (IACUC) of CHA University (IACUC240101), the Guide for the Care and Use of Laboratory Animals (National Institutes of Health, Bethesda, MD, USA), and the National Centre for the Replacement, Refinement and Reduction of Animals in Research (NC3Rs).

Acknowledgment

Not applicable.

Funding

This work was supported by the research grant of the Chungbuk National University Hospital in 2022.

Conflict of Interest

The authors declare no conflict of interest.

Supplementary Material

Supplementary material associated with this article can be found, in the online version, at https://doi.org/10.24976/Discov.Med.202638206.57.

References

[1] Chiu CW, Cheng H, Hsieh SL. Contusion Spinal Cord Injury Rat Model. Bio-protocol. 2017; 7: e2337. https://doi.org/10.21769/BioProtoc.2337.

[2] Baptiste DC, Fehlings MG. Pharmacological approaches to repair the injured spinal cord. Journal of Neurotrauma. 2006; 23: 318–334. https://doi.org/10.1089/neu.2006.23.318.

[3] Becker D, Sadowsky CL, McDonald JW. Restoring function after spinal cord injury. The Neurologist. 2003; 9: 1–15. https://doi.org/10.1097/01.nrl.0000038587.58012.05.

[4] Ko WK, Kim SJ, Han GH, Lee D, Jeong D, Lee SJ, *et al*. Transplantation of neuron-inducing grafts embedding positively charged gold nanoparticles for the treatment of spinal cord injury. Bioengineering & Translational Medicine. 2022; 7: e10326. https://doi.org/10.1002/btm2.10326.

[5] Qian T, Guo X, Levi AD, Vanni S, Shebert RT, Sipski ML. High-dose methylprednisolone may cause myopathy in acute spinal cord injury patients. Spinal Cord. 2005; 43: 199–203. https://doi.org/10.1038/sj.sc.3101681.

[6] Yates JR, Gay EA, Heyes MP, Blight AR. Effects of methylprednisolone and 4-chloro-3-hydroxyanthranilic acid in experimental spinal cord injury in the guinea pig appear to be mediated by different and potentially complementary mechanisms. Spinal Cord. 2014; 52: 662–666. https://doi.org/10.1038/sc.2014.118.

[7] Hall ED, Springer JE. Neuroprotection and acute spinal cord injury: a reappraisal. NeuroRx: the Journal of the American Society for Experimental NeuroTherapeutics. 2004; 1: 80–100. https://doi.org/10.1602/neurorx.1.1.80.

[8] Levitte S, Yarani R, Ganguly A, Martin L, Gubatan J, Nadel HR, *et al*. Case Series of Precision Delivery of Methylprednisolone in Pediatric Inflammatory Bowel Disease: Feasibility, Clinical Outcomes, and Identification of a Vasculitic Transcriptional Program. Journal of Clinical Medicine. 2023; 12: 2386. https://doi.org/10.3390/jcm12062386.

[9] Cho YK, Kim JH, Kim HS, Kim TO, Oh JH, Choi SC, *et al*. Randomised clinical trial: comparison of tegoprazan and lansoprazole as maintenance therapy for healed mild erosive oesophagitis. Alimentary Pharmacology & Therapeutics. 2023; 57: 72–80. https://doi.org/10.1111/apt.17255.

[10] Han GH, Kim SJ, Ko WK, Hong JB, Sheen SH, Cho MJ, *et al*. Anti-Inflammatory Effects of Tegoprazan in Lipopolysaccharide-Stimulated Bone-Marrow-Derived Macrophages. International Journal of Molecular Sciences. 2023; 24: 14589. https://doi.org/10.3390/ijms241914589.

[11] Liu J, Xu C, Chen L, Xu P, Xiong H. Involvement of Kv1.3 and p38 MAPK signaling in HIV-1 glycoprotein 120-induced microglia neurotoxicity. Cell Death & Disease. 2012; 3: e254. https://doi.org/10.1038/cddis.2011.140.

[12] Zhang Q, Liu L, Hu Y, Shen L, Li L, Wang Y. Kv1.3 Channel Is Involved In Ox-LDL-induced Macrophage Inflammation Via ERK/NF-κB signaling pathway. Archives of Biochemistry and Biophysics. 2022; 730: 109394. https://doi.org/10.1016/j.abb.2022.109394.

[13] Zhang X, Liang P, Zhang Y, Wu Y, Song Y, Wang X, *et al*. Blockade of Kv1.3 Potassium Channel Inhibits Microglia-Mediated Neuroinflammation in Epilepsy. International Journal of Molecular Sciences. 2022; 23: 14693. https://doi.org/10.3390/ijms232314693.

[14] Son M, Park IS, Kim S, Ma HW, Kim JH, Kim TI, *et al*. Novel Potassium-Competitive Acid Blocker, Tegoprazan, Protects Against Colitis by Improving Gut Barrier Function. Frontiers in Immunology. 2022; 13: 870817. https://doi.org/10.3389/fimmu.2022.870817.

[15] Jeon JY, Kim SY, Moon SJ, Oh K, Lee J, Kim B, *et al*. Pharmacokinetic Interactions between Tegoprazan and Metronidazole/Tetracycline/Bismuth and Safety Assessment in Healthy Korean Male Subjects. Clinical Therapeutics. 2021; 43: 722–734. https://doi.org/10.1016/j.clinthera.2021.01.026.

[16] Huang SM, Temple R, Throckmorton DC, Lesko LJ. Drug interaction studies: study design, data analysis, and implications for dosing and labeling. Clinical Pharmacology and Therapeutics. 2007; 81: 298–304. https://doi.org/10.1038/sj.clpt.6100054.

[17] Alsina-Sanchis E, Mülfarth R, Moll I, Mogler C, Rodriguez-Vita J, Fischer A. Intraperitoneal Oil Application Causes Local Inflammation with Depletion of Resident Peritoneal Macrophages. Molecular Cancer Research: MCR. 2021; 19: 288–300. https://doi.org/10.1158/1541-7786.MCR-20-0650.

[18] Kpemissi M, Metowogo K, Melila M, Veerapur VP, Negru M, Taulescu M, *et al*. Acute and subchronic oral toxicity assessments of *Combretum micranthum* (Combretaceae) in Wistar rats. Toxicology Reports. 2020; 7: 162–168. https://doi.org/10.1016/j.toxrep.2020.01.007.

[19] Mazzarino L, Loch-Neckel G, Dos Santos Bubniak L, Ourique F, Otsuka I, Halila S, *et al*. Nanoparticles Made From Xyloglucan-Block-Polycaprolactone Copolymers: Safety Assessment for Drug Delivery. Toxicological Sciences: an Official Journal of the Society of Toxicology. 2015; 147: 104–115. https://doi.org/10.1093/toxsci/kfv114.

[20] Ropper AE, Zeng X, Anderson JE, Yu D, Han I, Haragopal H, *et al*. An efficient device to experimentally model compression injury of mammalian spinal cord. Experimental Neurology. 2015; 271: 515–523. https://doi.org/10.1016/j.expneurol.2015.07.012.

[21] Abukhader MM. The effect of route of administration in thymoquinone toxicity in male and female rats. Indian Journal of Pharmaceutical Sciences. 2012; 74: 195–200. https://doi.org/10.4103/0250-474X.106060.

[22] Ahmed RU, Alam M, Zheng YP. Experimental spinal cord injury and behavioral tests in laboratory rats. Heliyon. 2019; 5: e01324. https://doi.org/10.1016/j.heliyon.2019.e01324.

[23] van Gorp S, Leerink M, Nguyen S, Platoshyn O, Marsala M, Joosten EA. Translation of the rat thoracic contusion model; part 2 - forward versus backward locomotion testing. Spinal Cord. 2014; 52: 529–535. https://doi.org/10.1038/sc.2014.73.

[24] Kim SJ, Ko WK, Jo MJ, Arai Y, Choi H, Kumar H, *et al*. Anti-inflammatory effect of Tauroursodeoxycholic acid in RAW 264.7 macrophages, Bone marrow-derived macrophages, BV2 microglial cells, and spinal cord injury. Scientific Reports. 2018; 8: 3176. https://doi.org/10.1038/s41598-018-21621-5.

[25] Schmittgen TD, Livak KJ. Analyzing real-time PCR data by the comparative C(T) method. Nature Protocols. 2008; 3: 1101–1108. https://doi.org/10.1038/nprot.2008.73.

[26] Peng Y, Lu K, Li Z, Zhao Y, Wang Y, Hu B, *et al*. Blockade of Kv1.3 channels ameliorates radiation-induced brain injury. Neuro-oncology. 2014; 16: 528–539. https://doi.org/10.1093/neuonc/not221.

[27] Jeffery ND, Brakel K, Aceves M, Hook MA, Jeffery UB. Variability in Open-Field Locomotor Scoring Following Force-Defined Spinal Cord Injury in Rats: Quantification and Implications. Frontiers in Neurology. 2020; 11: 650. https://doi.org/10.3389/fneur.2020.00650.

[28] Wu Q, Zhang Y, Zhang Y, Zhang W, Zhang W, Liu Y, *et al*. Riluzole improves functional recovery after acute spinal cord injury in rats and may be associated with changes in spinal microglia/macrophages polarization. Neuroscience Letters. 2020; 723: 134829. https://doi.org/10.1016/j.neulet.2020.134829.

[29] Roig SR, Estadella I, Cirera-Rocosa S, Navarro-Pérez M, Felipe A. Kv1. 3 In microglia: Neuroinflammatory determinant and promising pharmaceutical target. Journal of Neurology & Neuromedicine. 2018; 3: 18–23.